JOURNAL OF VIROLOGY, Sept. 2010, p. 9149–9160 Vol. 84, No. 18
0022-538X/10/$12.00 doi:10.1128/JVI.00642-10

Foot-and-Mouth Disease Virus Replicates Only Transiently in Well-Differentiated Porcine Nasal Epithelial Cells[▽]

Pradyot Dash,† Paul V. Barnett, Michael S. Denyer,‡ Terry Jackson, Catrina M. A. Stirling,§ Philippa C. Hawes, Jennifer L. Simpson, Paul Monaghan,¶ and Haru-H. Takamatsu*

Institute for Animal Health, Pirbright Laboratory, Pirbright, Woking, Surrey GU24 0NF, United Kingdom

Received 25 March 2010/Accepted 18 June 2010

Three-dimensional (3D) porcine nasal mucosal and tracheal mucosal epithelial cell cultures were developed to analyze foot-and-mouth disease virus (FMDV) interactions with mucosal epithelial cells. The cells in these cultures differentiated and polarized until they closely resemble the epithelial layers seen *in vivo*. FMDV infected these cultures predominantly from the apical side, primarily by binding to integrin αvβ6, in an Arg-Gly-Asp (RGD)-dependent manner. However, FMDV replicated only transiently without any visible cytopathic effect (CPE), and infectious progeny virus could be recovered only from the apical side. The infection induced the production of beta interferon (IFN-β) and the IFN-inducible gene Mx1 mRNA, which coincided with the disappearance of viral RNA and progeny virus. The induction of IFN-β mRNA correlated with the antiviral activity of the supernatants from both the apical and basolateral compartments. IFN-α mRNA was constitutively expressed in nasal mucosal epithelial cells *in vitro* and *in vivo*. In addition, FMDV infection induced interleukin 8 (IL-8) protein, granulocyte-macrophage colony-stimulating factor (GM-CSF), and RANTES mRNA in the infected epithelial cells, suggesting that it plays an important role in modulating the immune response.

Foot-and-mouth disease is an economically important disease caused by foot-and-mouth disease virus (FMDV), a picornavirus, belonging to the genus *Aphthovirus* and family *Picornaviridae*. Field strains of FMDV infect cells by attaching to integrin receptors through a highly conserved Arg-Gly-Asp (RGD) tripeptide motif which is located on a surface-exposed loop of VP1 (29). A number of different species of RGD-binding integrin (αvβ1, αvβ3, αvβ6, and αvβ8) have been reported to serve as receptors for infection (8, 22–24). However, αvβ6 is believed to function as the principal receptor for infection in the host (33). FMDV is highly infectious and can become established in susceptible animals by inhalation of relatively small levels of airborne virus (predominantly cattle) or ingestion of contaminated material (primarily pigs) (5). Apart from direct infection through injured skin or abrasion, the epithelial cells of the oral and upper respiratory tract mucosal surfaces are likely to be the first point of contact with the virus. In animals, FMDV undergoes early and rapid replication at the predilection sites in the pharynx and tonsil (5). This is followed by a viremic phase lasting 4 or 5 days, during which the virus spreads to other epithelial tissues and establishes itself at other secondary sites of replication (5). At these secondary sites, vesicles normally form, and the vesicles rupture to produce classical ragged-edge erosions. Although nasal mucosa has been suggested as a primary site of FMDV replication (26), there has been no evidence to support this claim (4). FMDV RNA can be detected in the nasal mucosa and trachea of pigs up to 4 days after infection; however, pathological signs of infection are not observed at these sites (3; P. Dash, unpublished observation).

Pigs are known to be more resistant to aerosol infection than cattle, though they excrete larger amounts of virus once infection is established (1, 2, 17, 38). The reason for the apparent reduced susceptibility to aerosol infection of pigs is unclear. Here we have investigated the interaction of FMDV with pig nasal and tracheal epithelial cells using polarized, differentiated three-dimensional (3D) cultures. The results provide insight into the possible reasons why pigs are relatively resistant to FMDV by aerosol challenge.

MATERIALS AND METHODS

Animals and tissue sample collection. Under Home Office project license PPL70/5859 and after euthanasia, tissue samples were collected and placed in cold phosphate-buffered saline (PBS) for subsequent culture from outbred pigs of either sex. The pigs weighed between 6 and 12 kg and were obtained from the Institute for Animal Health, Compton Laboratory. For reverse transcription-PCR (RT-PCR) and immunofluorescence analyses, the tissue samples were collected and placed in RNALater (Ambion) and 4% paraformaldehyde (PFA), respectively.

Reagents and antibodies. The components of seeding medium, growth medium, and differentiation medium were as follows. Seeding medium consisted of Dulbecco's modified essential medium (DMEM) and Ham's F12 medium mixture (1:1) containing 5% fetal calf serum (FCS), penicillin (200 U/ml), streptomycin (200 μg/ml), gentamicin (50 μg/ml), kanamycin (100 μg/ml), and amphotericin B (2.5 μg/ml). Growth medium consisted of DMEM and Ham's F12 medium mixture (1:1) containing 2% Ultroser G (Biosepra), cholera toxin (10 ng/ml) and the antibiotics/antimycotic for seeding medium. The differentiation medium is the same as growth medium and in addition contained retinoic acid (0.1 μg/ml). MDBK-t2 growth medium consisted of DMEM with 10% FCS,

* Corresponding author. Mailing address: Department of Immunology, Institute for Animal Health, Pirbright Laboratory, Pirbright, Woking, Surrey GU24 0NF, United Kingdom. Phone: 44 1483 231088. Fax: 44 1483 232448. E-mail: haru.takamatsu@bbsrc.ac.uk.

† Present address: Department of Immunology, St. Jude Children's Research Hospital, Memphis, TN.

‡ Present address: Department of Oncology, Postgraduate Medical School, University of Surrey, Guildford, Surrey, United Kingdom.

§ Present address: VMRD, Pfizer Ltd., Sandwich, Kent, United Kingdom.

¶ Present address: CSIRO Australian Animal Health Laboratory, 5 Portarlington Rd., East Geelong VIC 3219, Australia.

▽ Published ahead of print on 30 June 2010.

blasticidine S (100 μg/ml), penicillin (100 U/ml), streptomycin (100 μg/ml), and amphotericin B (2.5 μg/ml). The MDBK-t2 cell line, which is stably transfected with a chloramphenicol acetyltransferase (CAT) reporter gene cloned under the human Mx promoter (20), was a kind gift from Bryan Charleston, Institute for Animal Health, Compton, United Kingdom.

The Golgi marker anti-β-COP antibody (23C) has been described previously (32). The anti-FMDV monoclonal antibodies (MAbs) B2 and D9 have been described previously (30). The anti-FMDV 2C (clone 3F7) antibody was a kind gift from E. Brocchi (Instituto Zooprofilattico Sperimentale della Lombardia e dell'Emilia, Brescia, Italy). Anti-human αvβ8 (clones 14E5 and 37E1) has been previously described by Mu et al. (35). Other primary antibodies used were mouse anti-acetylated α-tubulin (6-11-B; Sigma), anti-human αvβ6 (clone 10D5; Chemicon), anti-human αvβ3 (clone LM609; Chemicon), and anti-human β1 (clone HB1.1; Chemicon), which are cross-reactive to pig integrins, rabbit antisera against ZO-1 (zonula occludens protein 1) and claudin, and mouse monoclonal antibodies against occludin (all from Zymed) and E-cadherin (BD Pharmingen). The secondary antibodies used for flow cytometry were phycoerythrin-conjugated anti-mouse IgG1 and IgG2a (Cambridge Biosciences). Secondary antibodies used for immunofluorescence were goat anti-mouse Alexa Fluor 488 or Alexa Fluor 568, goat anti-rat Alexa Fluor 568, goat anti-rabbit Alexa Fluor 488 (Invitrogen), and 4′,6′-diamidino-2-phenylindole (DAPI) for nuclear stain. All other reagents and chemicals, unless otherwise stated, were obtained from Sigma.

3D nasal and tracheal epithelial cell cultures. The 3D nasal mucosal epithelial (NME) and tracheal mucosal epithelial (TME) cell culture protocol was based on a modified method used for human airway epithelial cultures (49). Briefly, nasal and tracheal mucosae, including the cartilage from pigs from the Institute for Animal Health, Compton, United Kingdom, originating from the same herd and at the same age (4 weeks old) were washed four times in ice-cold Ca^{2+} Mg^{2+}-free phosphate buffered saline (PBSa) containing 5 mM dithiothreitol (DTT) and twice with ice-cold PBSa alone. After the mucosae were washed, they were removed from the cartilage and incubated at 4°C overnight in PBSa containing protease (type XIV; 0.4 mg/ml). The protease was inactivated (by adding FCS to a final concentration of 2.5%), and the small sheets of epithelial cells were dislodged by vigorous agitation. The cells were centrifuged at 500 × *g* for 10 min at 4°C and washed three times with seeding medium. Contaminating fibroblasts were removed by selective attachment to 9-mm petri dishes (BD Biosciences) for 30 to 60 min at 37°C. The cell suspension was collected, adjusted to 10^6 cells/ml in seeding medium containing cholera toxin (10 ng/ml), and seeded at a concentration of 10^5 cells/cm^2 onto Transwell tissue culture inserts (0.4-μm pore size; 6.5-mm membrane diameter; Corning) coated with rat tail collagen type I (5 μg/cm^2) and human fibronectin (5 μg/cm^2) (BD Biosciences). Twenty-four hours after incubation at 37°C, the medium was removed carefully and replaced with growth medium. After the cells were confluent, the medium was replaced with differentiating medium and the cells were brought to the air-liquid interface. Typically, 3-week-old cultures that were completely polarized and differentiated were used for the experiments after the integrity and polarity of the culture were checked by measurement of the transepithelial electrical resistance (TEER) using a VoltOhm meter (EVOM; World Precision Instruments) in accordance with the manufacturer's instructions. To examine the integrity of the 3D nasal epithelial culture layer, paracellular permeability was also examined using ^{51}Cr. To establish that the epithelial cells expressed the tight junction proteins zonula occludens (ZO-1), occludin, and adherens junction protein E-cadherin, the 3D cultures were examined by immunofluorescence using specific reagents.

Electron microscopy. Three-dimensional cultures were examined by scanning and transmission electron microscopy. Briefly, the cells on the 3D culture membrane were fixed with 2% glutaraldehyde for 1 h and then postfixed with 1% osmium tetroxide for 1 h. For scanning electron microscopy, the fixed membrane was removed from the insert, dehydrated by immersion in a series of acetone-water solutions (70% to 100%), dried, mounted, and sputter coated with gold particles (<10 nm). These samples were observed using an S-520 scanning electron microscope (Hitachi). For transmission electron microscopy (TEM), the fixed membrane was removed and dehydrated in an ethanol series (70% to 100%). After a propylene oxide wash, the samples were embedded in fresh epoxy resin and sectioned for TEM. The sections were imaged using the FEI Tecnai 12 with a TVIPS F214 digital camera.

Virus. The FMDV strain O1K (Kaufbeuren) cad2 was grown and titrated using primary epithelial cells derived from bovine thyroid (BTY) which is highly susceptible to field isolates of FMDV (40). The FMDV strain O1K cad2 is dependent on integrins as its sole receptor family (22). FMDV O1K cad2 grown on primary BTY cells was further purified using a sucrose density gradient (15), and the titer of the virus stock was determined to be 10^9 50% tissue culture infective doses ($TCID_{50}$)/ml. The virus was tested on CHO cells to confirm a lack of heparan sulfate binding (data not shown). The stock virus was diluted 100-fold for use in the infection experiments. The FMDV field strain OUKG/34/2001 (6) (isolated from the vesicular lesion of an infected pig; $10^{8.8}$ $TCID_{50}$/ml) was obtained from Zhidong Zhang, Institute for Animal Health, Pirbright, United Kingdom.

Integrin expression. Integrin expression of nasal and tracheal epithelial cells from pig tissue samples and 3D cultures was examined by flow cytometric analysis as described by Jackson et al. (24) with a minor modification. The epithelial cells from 3D culture were harvested by standard trypsinization and incubated for 30 min at 37°C, in 5% CO_2 prior to staining, to permit recovery and reexpression of membrane receptors on cells which might have been affected by the trypsinization process.

Competition assays for virus binding and infection. Virus binding and binding competition were both examined by a FACSCalibur (Becton Dickinson) using their CellQuest software, collecting at least 8,000 cells per sample by detecting cell surface-bound virus using an anti-FMDV VP1-specific MAb (clone B2) as described previously (28). For the binding competition experiment, competing MAbs (anti-human αvβ6 [clone 10D5]; anti-human αvβ3 [clone LM609] [10 μg/ml]) and peptides (RGD peptide [VPNLRGDLQVLAQKVAR] and RGE peptide [VPNLRGELQVLAQKVAR] [10 mM, 1 mM, 0.1 mM]) were used (24). For the infection competition experiment, 3D nasal mucosal epithelial cell cultures (6.5-mm membrane diameter inserts) were pretreated with peptide or antibody for 30 min, followed by the addition of purified O1K cad2 (multiplicity of infection [MOI] of ~3). The cultures were incubated for a further 30 min and acid washed (described below). The apical and basolateral media were collected at the 16-h time point and titrated on BTY cells to determine the level of reduction in the virus yield. Virus recovery in the presence or absence of competitors confirmed that this methodology was sufficient for the virus to enter polarized cells.

Viral inoculation of 3D nasal mucosal epithelial cultures. The cultures that showed a TEER reading of more than 300 Ω · cm^2 were selected for the infection experiments. The apical surfaces of the 3D cultures were rinsed three times with 500 μl of medium, and the cells were infected with 60 μl of viral suspension (MOI of ~3) for 1 h at 37°C. Infection of the basolateral surfaces of the cultures was performed by inverting the culture inserts and exposing the permeable support to a concentration of virus equivalent to that used for the apical inoculation. Following infection, the residual extracellular virus was inactivated by an acid wash buffer (saline [pH 5.2] containing 0.127 M acetic acid and 0.087 M sodium citrate) for 2 min. The physiological pH was restored by adding culture medium.

Assessment of progeny virus release. To assess the release of progeny virus, 500 μl of medium was added to the apical surface of the infected culture 30 min prior to the predetermined time points, and the cultures were returned to the 37°C incubator. At the required time point, 500 μl of apical wash and 1 ml of basolateral medium was collected and stored at −70°C until assayed for virus on primary BTY cells and expressed as log $TCID_{50}$.

Confocal microscopy. The 3D cultures in the inserts (with or without infection) were fixed in 4% PFA for 1 h at room temperature. The cultured inserts were rinsed thrice in PBS. The cells were permeabilized with 0.1% Triton X-100 in PBS for 15 min, incubated in PBS containing 0.5% bovine serum albumin (BSA), and labeled by the addition of a primary antibody for 1 h. For immunofluorescence labeling of the tissue samples, PFA-fixed tissue samples were cut to a thickness of 50 to 100 μm using a vibrating microtome (Leica Microsystems, United Kingdom). Fixed and permeabilized tissue sections were labeled as described above. Both cultured inserts and the tissue sections were washed with PBS and further stained with a secondary antibody conjugated to Alexa Fluor. After the final wash, the nuclei were stained with DAPI. After the final staining step, the membrane was cut from the insert and mounted onto slides using Fluoromount G and coverslips. The tissue sections were mounted onto slides with a gene frame (Thermo Life Sciences) using Fluoromount G and coverslips and imaged by using a Leica TCS SP2 confocal microscope.

Domain-selective cell surface labeling and Western blot analysis. The surfaces of the 3D nasal mucosal epithelial cell cultures were labeled with biotin at its apical or basolateral domain using the method described by Tugizov et al. (45). For identifying the domain localization of αvβ6 integrin, the cell lysate was immunoprecipitated with 2 μg of anti-αvβ6 antibody and captured with protein A/G beads. Western blotting was performed with neutravidin-horseradish peroxidase (HRP). For detection of β1 integrin, the biotinylated cell lysates were precipitated with avidin-agarose (Pierce), and the Western blot was probed with anti-β1 integrin, followed by anti-mouse antibody conjugated to HRP. The blots were developed using enhanced chemiluminescence (ECL) reagents (Amersham Biosciences).

RNA isolation, reverse transcription, and PCR. The total cellular RNA (from both cultures and tissue samples) was extracted using an RNAqueous kit (Ambion), and the DNA contamination from the RNA preparation was removed using a DNA-free kit (Ambion) per the manufacturer's instructions. Reverse transcription was carried out with 2 μg of total RNA and an oligo(dT) primer, using Improm II reverse transcriptase (Promega) per the manufacturer's instructions. The cDNA was then used for PCR amplification with GoTaq polymerase system (Promega) or Master kit (Applied Biosystems, United Kingdom) for quantitative PCR using the appropriate primers. The primers used were as follows. For FMDV 2B, the forward primer was 5′AAGGAATTCGGGCCCT TCTTTTTCTCCGACGTTA3′, and the reverse primer was 5′CTGTTTCTCT GCTCTCTCAAG3′. For porcine alpha interferon (IFN-α), the forward primer was 5′ATGGCCCCAACCTCA-GCCTTC3′, and the reverse primer was 5′TC ACTCCTTCTTCCTGAGTCT3′. For porcine IFN-β, the forward primer was 5′ATGGCTAA-CAAGTGCATCCTC CAA3′, and the reverse primer was 5′T CAGTTCCGGAGGTAATCTGTAAG3′. For porcine beta-actin, the forward primer was 5′GAGAAGCTGTGCTACGTCGC3′, and the reverse primer was 5′CCAGACAGCACTGTGTTGG-C3′. For Mx1, the forward primer was 5′G AACTGATCAAGGAGGAA3′, and the reverse primer was 5′GCATCTTGTC ACAA TTCC3′. For granulocyte-macrophage colony-stimulating factor (GM-CSF), the forward primer was 5′CATGTGGSTGCCATCAAAGAAGCCC3′, and the reverse primer was 5′TGGG-TTTCACAGGAAGTTTCCTCGG3′. For RANTES (regulated upon activation, normal T-cell expressed and secreted), the forward primer was 5′ATGAAGGTCT CCACCGCTG-CCCTTGC3′, and the reverse primer was 5′CTAGCTCAACTCCAAGGAGTTGATG3′.

Quantitative real-time RT-PCR assays to detect viral RNA were performed as described previously (52). Conversions of viral RNA and IFN mRNA to copy number/cell were made with the assumption that a cell, on average, contained approximately 6 pg of total RNA, which has been used to express the tissue content of FMDV RNA (3).

The primers and probes used were a kind gift from Zhidong Zhang (Institute for Animal Health, Pirbright, United Kingdom) and were as follows. For porcine IFN-α, the forward primer was 5′GCCTCCTGCACCAGTTCTACA3′, the reverse primer was 5′TGCATGACACAGGCTTCCAG3′, and the probe was FAM-TCCCTGAGCTGCTGATCCAGTCCA3′, where FAM is 6-carboxyfluorescein. For porcine IFN-β, the forward primer was 5′GCGTGGAATGAAAC CGTCATT3′, the reverse primer was 5′CCAGGATTGTCTCCAGGTCATC3′, and the probe was FAM-TCTGCCCATCAAGTTCCACAAGGATAGTCT. For FMDV internal ribosome entry site (IRES), the forward primer was 5′CC GAGTGTCGCGTGTTACCT3′, the reverse primer was 5′AACCACTGGTGA CAGGCTAAGG3′, and the probe was FAM-TGCCCTTTAGGTACCC. For glyceraldehyde-3-phosphate dehydrogenase (GAPDH), the forward primer was 5′GCATCGTGGAGGGAC-TTATGA3′ , the reverse primer was 5′GGGCCA TCCACAGTCTTCTG3′, and the probe was FAM-CACTGTC-CACGCCAT-CACTGCCA.

Antiviral activity of FMDV-infected supernatant. To eliminate any residual infectious virus, the apical and basolateral media from the 3D nasal mucosal epithelial cell cultures (4.2-cm^2 membrane diameter inserts) infected with FMDV were treated with 5 N HCl to lower the pH to 2 (approximately 10 μl/500 μl of media) for 30 min on ice, which was more than optimal, given that FMDV is extremely acid labile (11). Following disruption of any virus present, the pH was restored by the addition of 5N NaOH (until the medium changed back to its original color). The treated apical and basolateral media were diluted 5 times with MDBK-t2 growth medium and examined for the presence of type I IFN activity by a Mx-CAT reporter assay using the MDBK-t2 cell line as described previously (27).

Porcine IL-8 ELISA. Interleukin 8 (IL-8) in both the apical and basolateral media of infected or control 3D nasal mucosal epithelial cell cultures was measured using a porcine IL-8 enzyme-linked immunosorbent assay (ELISA) kit (Biosource) per the manufacturer's instructions.

Statistical analysis. The data were expressed as the means ± standard errors of the means (SEMs). Differences between treatments were assessed using a two-tailed Student's *t* test for paired observations. A P value of <0.05 is considered statistically significant.

RESULTS

Establishment and characterization of 3D porcine nasal and tracheal epithelial cell cultures. Well-differentiated polarized 3D cultures of nasal and tracheal mucosal epithelial cells were established by adapting the method for human airway epithelial cultures (49). Morphological examination of these cultures revealed pseudostratified mucociliary epithelial structures with an appearance that closely resembled those *in vivo* (Fig. 1) and were uniform between the different batches grown. After 5 to 7 days of culture under an air-liquid interface, large parts of the apical surfaces were covered with constantly beating cilia, observed by phase-contrast microscopy (results not shown). To assess the purity of epithelial cell culture, potentially contaminated nonepithelial cells were identified by vimentin staining, as vimentin is expressed in cells of mesenchymal origin, including fibroblasts but generally not expressed in epithelial cells (41). Vimentin staining demonstrated that almost all of the cells in the cultures were devoid of fibroblast contaminants (Fig. 1H). Examination of 3- to 4-week-old 3D nasal and tracheal epithelial cell cultures by histological sections and electron microscopic analysis revealed that these

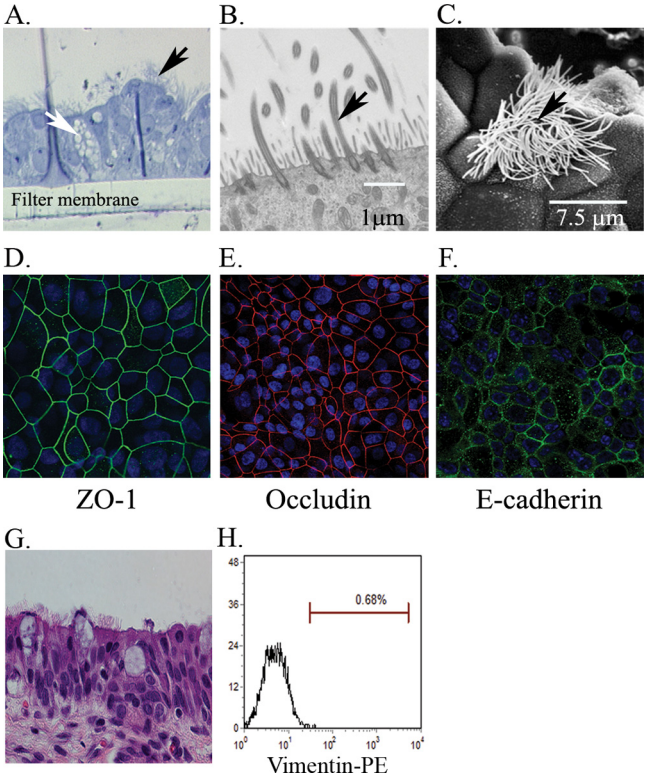

FIG. 1. Differentiation and polarization of porcine nasal mucosal epithelial (NME) and tracheal mucosal epithelial (TME) cells in 3D cultures. Porcine nasal and tracheal epithelial cells were seeded onto collagen/fibronectin-coated porous inserts and cultured for 3 to 4 weeks. (A to C) Toludine blue staining (A) (3D NME), transmission electron microscopy (B) (3D NME), and scanning electron microscopy (C) (3D TME) demonstrate cilia (black arrow) and goblet cells (white arrow) in the differentiated epithelial culture. (D to F) In 3D NME cultures, expression analysis of tight and adherent junction marker proteins ZO-1 (D) shown in green, occludin (E) shown in red, and E-cadherin (F) shown in green demonstrate that these epithelial cells are polarized. Cell nuclei were stained with DAPI (blue). (G) A hematoxylin-and-eosin-stained section of a pig nasal mucosal tissue sample is also shown for comparison. (H) Dissociated cells from 3D NME cultures analyzed by a flow cytometer demonstrate no fibroblast cell contamination detected by the fibroblast cell marker vimentin. Panel H indicates that vimentin-positive cells were <3% in the 3D NME culture.

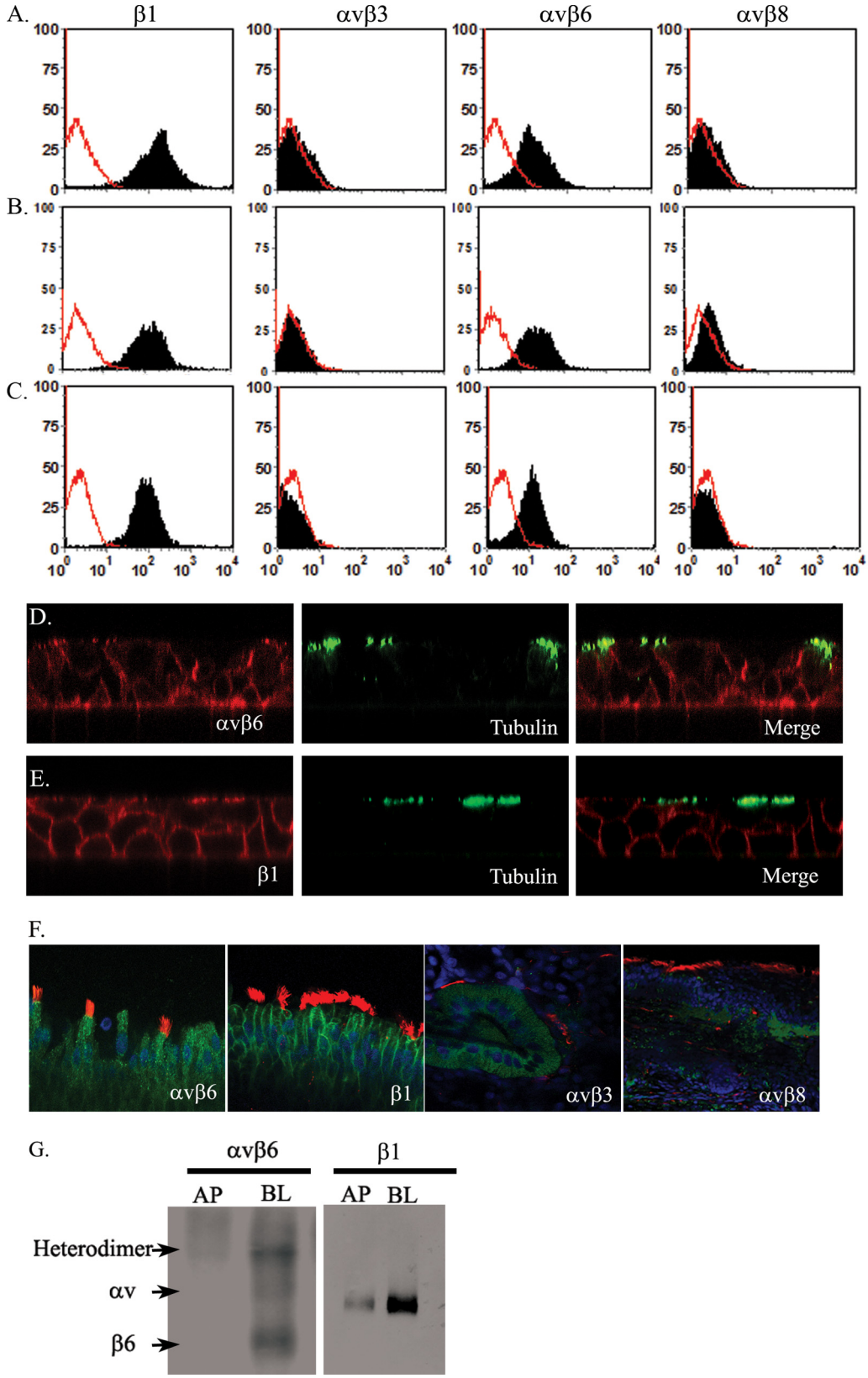

FIG. 2. Porcine nasal and tracheal epithelial cells express integrin αvβ6. Flow cytometric analysis of integrin expression on the epithelial cells isolated from 3D cultured pig nasal epithelial cells (A), pig nasal tissue samples (B), and trachea samples (C). From right to left, epithelial cells were analyzed for their expression of β1 (MAb HB1.1), αvβ3 (MAb LM609), αvβ6 (MAb 10D5), and αvβ8 (MAbs 37E1 and 14E5). Each integrin staining is shown as a black histogram, and the background staining is shown as a red line. A representative result of three independent experiments is shown.

cultures were composed of a number of different epithelial cell subtypes, including ciliated and nonciliated cells and possibly mucin-producing goblet cells (Fig. 1A, B, and C). The cultures also expressed the tight junction (zonula occludens protein 1 [ZO-1] and occludin) and adherens junction (E-cadherin) proteins, indicating that the cells were polarized (Fig. 1D to F). The transepithelial electrical resistance (TEER) reached a stable resistance of about 900 to 1,500 $\Omega \cdot cm^2$ around day 10 after seeding, demonstrating intracellular junction development (see Fig. 4B). The integrity of the 3D cultured epithelial layers was further demonstrated by a paracellular permeability assay, as no radioactivity was detected in the basolateral chamber after 30 min of incubation with medium containing radioactive ^{51}Cr applied at the apical chamber (data not shown).

Porcine nasal and tracheal epithelial cells express integrin αvβ6, and FMDV binding to the epithelial cells is RGD dependent. Expression of the known FMDV RGD-binding integrin receptors on 3D cultured porcine nasal and tracheal mucosal epithelial cells was examined by flow cytometry, confocal microscopy, and domain-selective labeling and immunoprecipitation analysis. Flow cytometry of dissociated epithelial cells from 3-week-old cultures showed expression of integrin αvβ6 but not integrins αvβ3 and αvβ8 (Fig. 2A). The expression of integrin β1 was strongly positive. Porcine nasal and tracheal mucosal epithelial cells, freshly isolated from animals, showed the same integrin expression profile (Fig. 2B and C) as the 3D cultures, confirming that the expression of αvβ6, αvβ3, and αvβ8 was not altered during culture. Consistent with the above observations, immunofluorescence microscopy analysis of 3-week-old 3D cultures (Fig. 2D and E) and sections of nasal mucosal tissue samples, freshly isolated from healthy pigs, also showed expression of integrins αvβ6 and β1 but were negative for integrins αvβ3 and αvβ8 in respiratory epithelial cells (Fig. 2F). Although the integrin αvβ6 was expressed on the apical side of the polarized cells which included some ciliated cells (identified by an anti-acetylated α-tubulin MAb) (Fig. 2D), it was more strongly expressed at the basolateral side. Integrin β1 expression, used in this study as a control, was expressed mostly on the lateral side and weakly on the apical side, but not on the basal side of the nasal mucosal epithelial cells (Fig. 2E). Although the αvβ3 and αvβ8 integrins were not detected on mucosal epithelial cells in the 3D cultures, weak expression of both αvβ3 and αvβ8 on the cells in the lamina propria of the nasal mucosa was observed from the tissue samples obtained from healthy pigs (Fig. 2F).

Uninfected 3D nasal epithelial cells were selectively labeled with biotin, either at the apical or basolateral surfaces of the polarized epithelial cells, by a domain-selective labeling assay. The labeled cells were lysed and immunoprecipitated with anti-integrin antibodies and then blotted with neutravidin-HRP. This confirmed that αvβ6 and β1 integrins were expressed more strongly on the basolateral side of the 3D NME cultures (Fig. 2G).

Next we investigated whether αvβ6 on the nasal and tracheal mucosal epithelial cell cultures was used as a receptor for FMDV. Binding of FMDV strain O1K cad2 to porcine nasal mucosal epithelial cells from 3D cultures was demonstrated by flow cytometry, and this binding was inhibited by an RGD-containing peptide in a concentration-dependent manner, but not by the control RGE version of this peptide (Fig. 3A). Virus binding was also inhibited by the anti-αvβ6 MAb, but not by the anti-αvβ3 MAb (Fig. 3B), confirming αvβ6 as the major receptor for virus attachment on these cells. FMDV infection was also examined with intact 3D cultures in the presence of an RGD peptide or anti-αvβ6 MAb. The cultures were infected with O1K cad2, and the amount of infectious virus recovered from the 3D cultures 16 h after infection was determined. Virus recovery was reduced by 50% in the presence of the RGD peptide (Fig. 3C) and by 35% in the presence of the anti-αvβ6 MAb compared with the control (Fig. 3D).

FMDV replicates in 3D cultures without CPE. When 3D nasal mucosal epithelial cultures were infected with FMDV, a cytopathic effect (CPE) was not observed at any time point. Therefore, we examined whether FMDV was able to replicate in the cultures by detection of viral RNA using quantitative RT-PCR for the IRES and by confocal microscopy detection of the nonstructural protein 2C. In the 3D nasal mucosal epithelial cultures, viral RNA was detected 4 h postinfection and rapidly disappeared thereafter (Fig. 3E). Similar results were observed with the 3D tracheal mucosal epithelial cultures, but the peak of viral RNA production was greater and the viral RNA persisted longer (Fig. 3F). Confocal microscopy showed that FMDV nonstructural protein 2C was detected in nasal epithelial cells 3 h after apical infection (Fig. 3G, H, and I). Figure 3G and H show the horizontal section of FMDV-infected 3D nasal mucosal epithelial culture and that nonstructural protein 2C was present in the majority of the cells (Fig. 3H). An example of the image for an orthogonal section of an FMDV-infected 3D culture is shown in Fig. 3I. This shows that 2C was mainly localized at the apical side of columnar cells (Fig. 3I). In contrast, little or no 2C was detected on the basal side of the cells.

To test for the presence of infectious virus, media from the apical and basolateral surfaces of infected cultures were collected at various time points after apical infection and titrated on primary BTY cells. Infectious virus was detected only in 3D nasal mucosal epithelial cultures 4 to 24 h postinfection, not after 48 h postinfection (Fig. 3J). These observations were in agreement with the quantitative RT-PCR results (Fig. 3E). In the 3D tracheal mucosal epithelial cultures, infectious virus

(D and E) Confocal microscopic examination of αvβ6 (D) and integrin β1 chain (E) expression (in red) in a 3D NME culture shown as an orthogonal section. The cilia are shown in green, stained with anti-acetylated α-tubulin antibody. (F) Confocal images of the β1 chain and αvβ6, αvβ3, and αvβ8 (green) on nasal tissues. The αvβ6 and β1 integrins were expressed on mucosal epithelial cells, whereas weak expression of αvβ3 and αvβ8 was observed mainly on tubular epithelial cells of the lamina propria. (G) The expression of αvβ6 and β1 integrins was also demonstrated by biochemical analysis. The surfaces of 3D NME cultures were selectively labeled with biotin, either at the apical (AP) or basolateral (BL) side, lysed, immunoprecipitated with anti-αvβ6 (MAb 10D5) and blotted with neutravidin-HRP, or immunoprecipitated with avidin-agarose, which was followed by Western blotting with a β1-specific MAb (HB1.1).

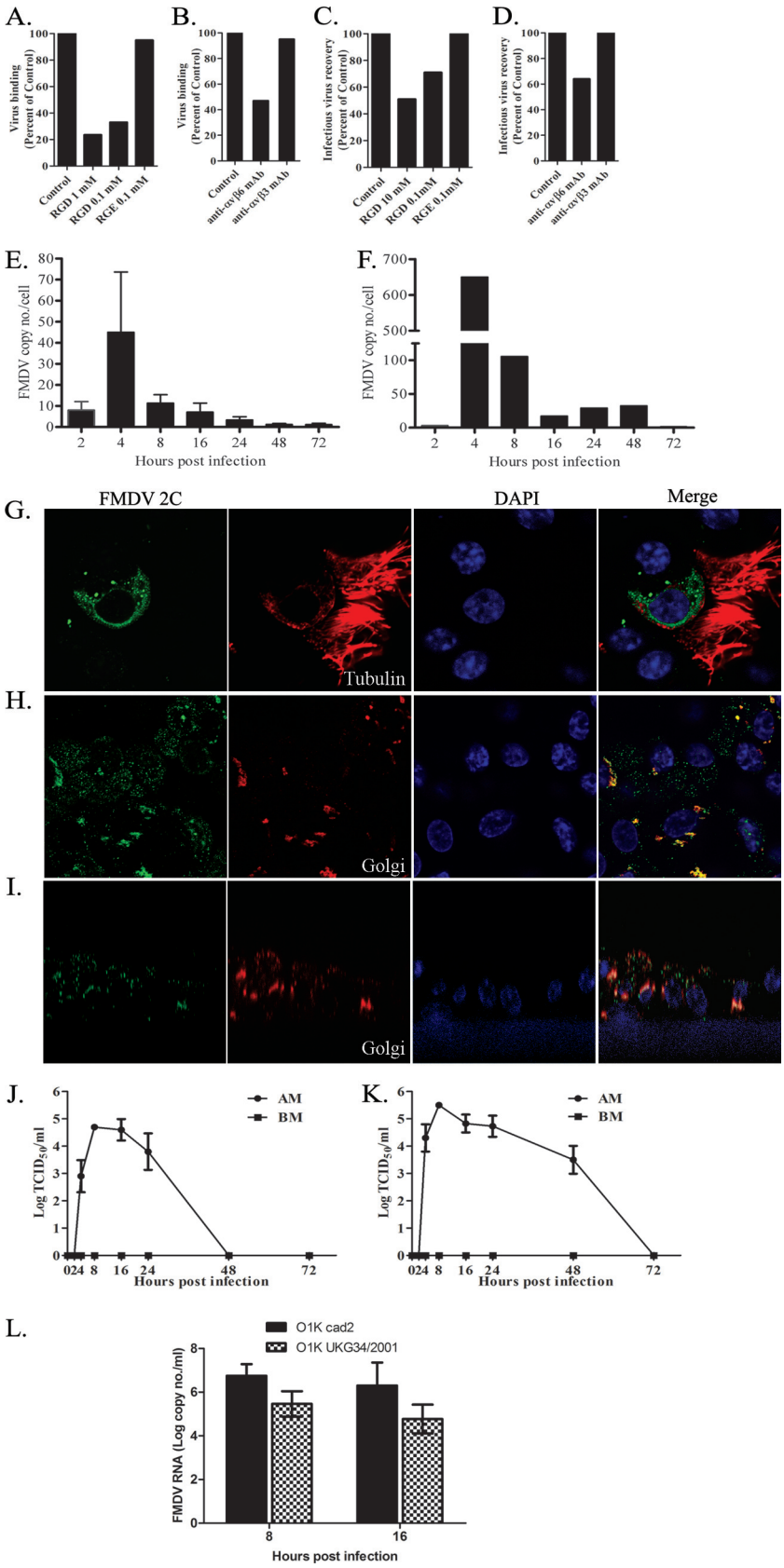

FIG. 3. FMDV binds to porcine nasal mucosal cells via the αvβ6 integrin using its RGD motif, replicates mainly at the apical side of the cells, and releases progeny virus in a polarized manner. (A and B) The binding of FMDV to dissociated epithelial cells from 3D cultures was inhibited

was recovered up to 48 h after apical infection, but not after this time point (Fig. 3K), again reflecting the results of quantitative RT-PCR (Fig. 3F). Virus was not detected at the basolateral side of 3D nasal or tracheal epithelial cultures at any time points sampled (Fig. 3J and K). To examine whether the lack of CPE and transient replication is specific to the FMDV O1K cad2 strain, we infected 3D nasal mucosal epithelial cultures apically with FMDV OUKG/34/2001 virus that had been isolated from a lesion in an infected pig (6). As shown in Fig. 3L, there was no appreciable difference between these two viruses in terms of replication rate and level of virus recovered, and no CPE was observed.

As the FMDV receptor αvβ6 was observed to be expressed more strongly at the basolateral surfaces of the 3D cultures, the ability of FMDV to infect through the basolateral route was examined. Nasal mucosal epithelial 3D cultures were infected either at the apical (as the positive control) or basolateral surfaces, and media from the apical and basolateral chambers were collected 8, 16, 24, 48, 72, and 96 h postinfection for virus detection by titration on primary BTY cells. Fresh cell culture media were added back to the inserts after each time point of sampling so that the data represented virus that had accumulated in supernatants since the previous time point of sampling. As demonstrated previously, when the cells were infected by the apical route, virus was recovered only from the apical media 8, 16, and 24 h postinfection, and no virus could be recovered from the basolateral media (Fig. 4A). When the cells were infected from the basolateral side, infectious FMDV was recovered from the apical side 16 h and 24 h though with a lower titer than that seen from infection through the apical route and only at 8 h postinfection from the basolateral side (Fig. 4A). In all of the above experiments, the 3D cultures did not show any visual CPE (Fig. 4E to H) normally characteristic of an FMDV infection in BHK cells or primary cells, such as BTY cells (Fig. 4C and D).

Undifferentiated epithelial cells are more susceptible to FMDV infection. FMDV is known to efficiently infect and replicate in conventional monolayer cultures (40), causing extensive CPE (14). Therefore, the effect of differentiation of porcine nasal mucosal epithelial cells on FMDV susceptibility was investigated. Collagen- and fibronectin-coated inserts, with a 0.33-cm^2 surface area, were seeded with freshly prepared nasal mucosal epithelial cells from healthy pigs and subsequently infected with FMDV O1Kcad2 at a MOI of ~3 at various days after seeding. After 1 h of incubation with virus, the cells were acid washed to inactivate virus that had not been internalized. The TEER was recorded before each experiment to assess the degree of differentiation and integrity of the epithelial layer. The supernatants from both the apical and basolateral chambers were collected 12 h postinfection and stored at −70°C. At the end of the experiment (day 25), the stored samples were titrated on BTY cells to detect the presence of infectious virus. Virus was recovered from both the apical and basolateral media of FMDV-infected cultures that had been seeded between 2 and 15 days earlier (Fig. 4B). Virus recovery peaked on day 5 after cell seeding (Fig. 4B), and thereafter, the virus yield from both apical and basolateral medium started to decrease. This reduction in virus yield continued for 15 days or more to a point where virus was no longer detected from the basolateral side (Fig. 4B).

FMDV induces IFN-β, Mx1, IL-8, RANTES, and GM-CSF in 3D nasal epithelial cultures. The results described above demonstrated that FMDV infects and replicates in 3D nasal and tracheal mucosal epithelial cultures, but only transiently and without any visible CPE. To understand the mechanisms that limit replication in the porcine nasal 3D cultures, we first investigated type 1 IFN. Both quantitative RT-PCR and standard RT-PCR were performed for the detection of type I IFN mRNA using total RNA isolated at different time points postinfection. IFN-β mRNA was induced only between 4 and 24 h postinfection (Fig. 5A and B), coinciding with the disappearance of the FMDV RNA (Fig. 5C). Antiviral GTPase enzyme Mx1 gene mRNA, which is induced by IFN, was also detected 16 h postinfection onwards (Fig. 5A). In contrast, IFN-α from 3D cultures was detected in both infected and uninfected cultures throughout the assay (Fig. 5A). Interestingly, IFN-α mRNA expression was observed in the majority of freshly isolated nasal epithelial tissue samples from healthy pigs, but not from snout tissue samples (data not shown).

The antiviral activity in the apical and basolateral media collected from the FMDV-infected 3D NME cultures at 8, 24, and 48 h postinfection, was also analyzed using an Mx-CAT reporter assay. At 24 h postinfection, significant ($P < 0.047$) antiviral activity was observed in the apical media by the CAT reporter assay compared to the negative-control uninfected culture supernatant (Fig. 5D).

Expression of the RANTES and GM-CSF mRNA and of IL-8 protein in FMDV-infected 3D NME cultures was also examined by RT-PCR and ELISA, respectively. RANTES mRNA was expressed only during early infection at 8 and 16 h

by RGD peptides (A) in a dose-dependent manner and by an anti-αvβ6 MAb (B), but not by an RGE peptide (A) or an anti-αvβ3 MAb (B). (C and D) FMDV infection and virus recovery from intact 3D cultures were also inhibited by RGD peptides (C) and an anti-αvβ6 MAb (D), but not by an RGE peptide (C) or an anti-αvβ3 MAb (D). These experiments were carried out in duplicate, and the mean data from two independent experiments are shown (these values are within 5% of each other). (E and F) Quantitative real-time RT-PCR of the FMDV IRES region at various time points postinfection. (E) 3D NME culture. The values are means plus standard errors (SE) (error bars) ($n = 4$ for all time points except $n = 3$ for 8 and 72 h). (F) 3D TME culture. The data shown here are representative of two independent experiments. (G to I) Confocal microscopy of FMDV nonstructural protein 2C (green) is shown. FMDV nonstructural protein 2C in ciliated cells (G) (cilia shown in red) and the wider spread of infection in 3D cultures (H) are shown. (I) An orthogonal section showing FMDV 2C (green) mostly located in the apical compartment. The Golgi apparatus is shown in red in panels H and I. (J and K) Graphs of infectious virus release to the FMDV-infected 3D culture supernatants (apical side [apical membrane {AM}] and basolateral side [basolateral membrane {BM}]) at various times postinfection. (J) 3D NME cultures (mean ± SE [error bar]) ($n = 3$). (K) 3D TME cultures (mean ± SE [error bar]) ($n = 3$). (L) Replication of field isolate OUKG34/2001strain compared to that of strain O1K cad2 in 3D NME cultures by quantitative RT-PCR is shown (mean ± SE) ($n = 3$). At both 8 h and 16 h postinfection, the copy numbers of FMDV IRES were not significantly different between the two strains of FMDV, though the OUKG34/2001 strain showed a lower copy number than the O1K cad2 strain did.

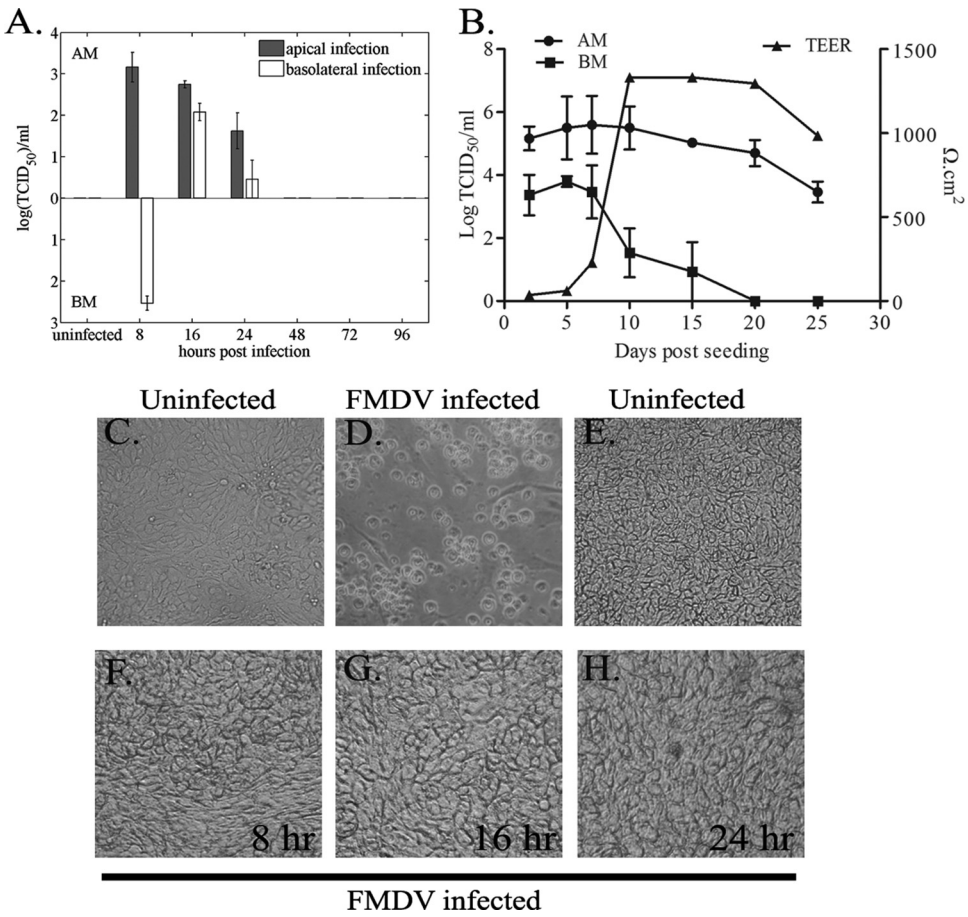

FIG. 4. Preferential infection and release of FMDV from the apical side in 3D nasal mucosal epithelial (NME) cultures without CPE depend on epithelial cell differentiation. (A) The 3D NME cultures were infected for 1 h with purified FMDV O1K cad2 at a MOI of ~3 through the apical membrane (AM) or basolateral membrane (BM) and then acid washed. Media from both apical and basolateral chambers were collected at various time points, and at each time point, the medium was replaced; therefore, the data represent the titer of virus that accumulated in the medium since the previous time sampling. The filled bars indicate FMDV recovered from the apical infection, and open bars indicate FMDV recovered from the basolateral infection. Data are mean ± standard errors (error bars) from four independent experiments. (B) When cells are infected apically, FMDV can be recovered from the basolateral chamber (BM) in undifferentiated 3D NME cultures, and the FMDV values are negatively correlated with the TEER values. Virus recovery from the apical side (AM) is also shown. Results are shown as means ± standard errors from three independent experiments. (C to H) FMDV infection induced a widespread cytopathic effect (CPE) in primary bovine thyroid epithelial cells (uninfected cells [C] and cells infected for 24 h [D]), but CPE was not observed in 3D NME cultures (uninfected cells [E] and in cells infected for 8 h [F], 16 h [G] or 24 h]H]). Images were observed by light microscopy, and photographs were taken using a Kodak digital camera.

(Fig. 6A), whereas GM-CSF mRNA was detected at all the time points (i.e., 2, 8, 16, 24, and 48 h), but not in mock infection controls (Fig. 6A). Although IL-8 protein was detected in both mock-infected and FMDV-infected cultures 8, 24, and 48 h postinfection, the FMDV-infected culture showed an increase of IL-8 over the same time points in the apical media, while the IL-8 concentration in mock-infected culture remained more or less constant. The quantity of IL-8 in the basolateral media increased over time points both in mock- and FMDV-infected 3D cultures, though the concentration was higher in the infected cultures (Fig. 6B).

DISCUSSION

For the first time we have developed monotypic 3D porcine epithelial cultures and applied this advantage toward a better understanding of the interaction between FMDV and porcine nasal and tracheal epithelium. The cells cultured three dimensionally are differentiated and polarized, and unlike conventional monolayer cultures, they closely resemble the structures and microenvironments observed *in vivo* (37). Such properties have led to the use of 3D cultures in wider areas of research, including microbiology and immunology in humans and other species (14, 18, 19, 25, 31, 36, 43, 50, 51). Recently, a short-term organotypic explant culture of porcine nasal mucosa that was used for studies on herpesvirus and porcine influenza virus has been reported (21), but not 3D cultures to our knowledge.

Using wild-type FMDV strains in our studies, our results confirmed that of the four known integrins (αvβ6, αvβ8, αvβ3, and αvβ1) that are used by FMDV to gain entry into the cells (8, 22–24), porcine nasal and tracheal mucosal epithelial cells, both *in vivo* and *in vitro*, express the αvβ6 heterodimer, but not αvβ3 or αvβ8. However, despite detection of β1 integrin in these cells, expression of αvβ1 could not be confirmed due to

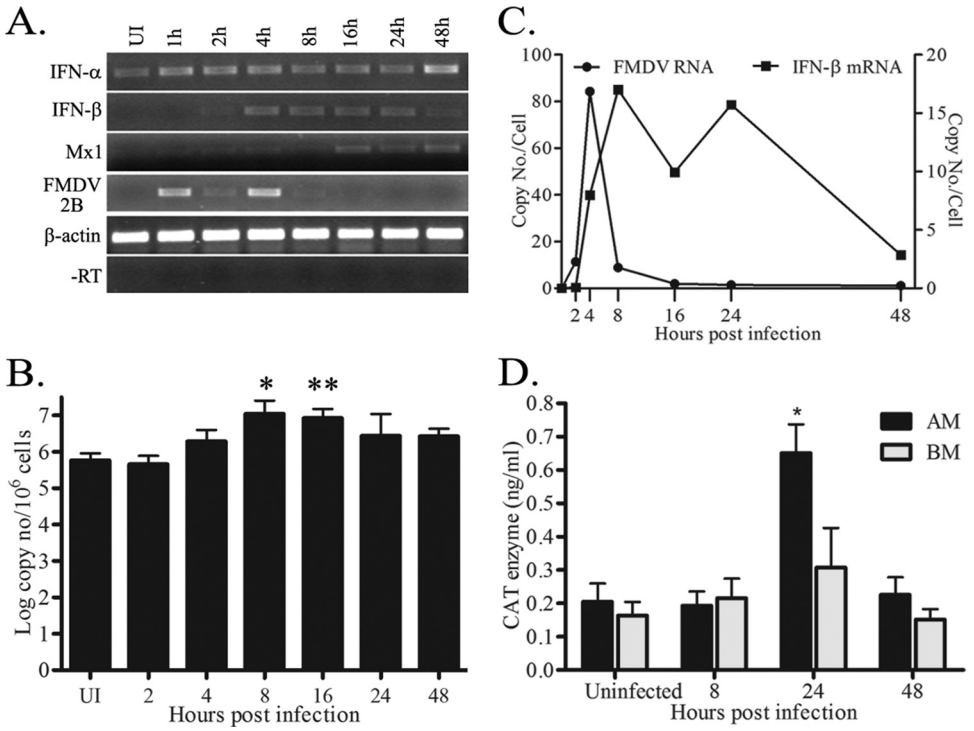

FIG. 5. Interferon responses to FMDV infection of 3D nasal mucosal epithelial (NME) cultures. (A) A representative figure of a standard RT-PCR for IFN-α, IFN-β, Mx1, and FMDV nonstructural protein 2B RNA demonstrates the disappearance of FMDV RNA coinciding with the induction of IFN-β mRNA, followed by expression of interferon-inducible protein Mx1 mRNA. Beta-actin and −RT (no reverse transcriptase) were included as positive and negative controls, respectively. (B) Quantitative real-time RT-PCR of IFN-β mRNA in FMDV-infected 3D NME cultures confirms the increase of IFN-β mRNA following FMDV infection (*, $P = 0.02$ for uninfected [UI] cells versus cells infected for 8 h; **, $P = 0.01$ for UI cells versus cells infected for 16 h). The data are shown as mean plus standard errors (error bars) from 4 separate experiments. The copy numbers were calculated as described in Materials and Methods and expressed as the log copy number per million cells. (C) A representative figure of the relationship between viral RNA and IFN-β mRNA, as examined by quantitative real-time RT-PCR from four independent experiments is depicted. (D) Antiviral activity in the supernatants from FMDV-infected 3D NME cultures was examined using an Mx-CAT assay as described in Materials and Methods. The black bars show data for cells collected from the apical side (apical membrane [AM]), while the gray bars show data for cells collected from the basolateral side (basolateral membrane [BM]). Data are shown as mean plus standard errors from three independent experiments. The value for cells infected for 24 h from the basolateral membrane was significantly different from the value for uninfected cells ($P = 0.047$) and is indicated by an asterisk.

the unavailability of the specific reagent for this heterodimer. The epithelium-specific expression of integrin αvβ6 in both cattle and sheep (10, 33) has identified this integrin as the most likely primary receptor for infection *in vivo* (33). Indeed, binding studies with FMDV O1K cad2 in the presence of peptides and anti-integrin MAbs showed that FMDV attaches to the nasal mucosal epithelial cells mostly via αvβ6 in a RGD-dependent manner (Fig. 3A to D). Thus, the lower susceptibility of pigs to FMDV by the inhalation route is unlikely to be related to a lack of FMDV receptors on the surfaces of nasal or tracheal mucosal epithelial cells.

Interestingly, FMDV replicates only transiently in these 3D nasal and tracheal epithelial cell cultures (Fig. 3E to K), without showing any evidence of extensive CPE (Fig. 4E to H). The infectious progeny virus was detected only from the apical side between 4 and 24 h in 3D nasal mucosal epithelial cultures and between 4 to 48 h in 3D tracheal mucosal epithelial cultures (Fig. 3J and K) postinfection, but not in basolateral media at any time point, indicating a directional release of the FMDV in polarized epithelial cells. This directional release of FMDV was also demonstrated from the experiments infecting 3D cultures from the basolateral side (Fig. 4A), where the density of integrin αvβ6 expression is highest (Fig. 2D and F). These results indicate that FMDV is predominantly released from the apical side in a polarized manner, irrespective of the route of infection, as has been observed with several other viruses (13, 39, 44, 47, 50, 51). Though we do not have an explanation for why FMDV is preferentially released from the apical side, the difference in susceptibility between the apical and basolateral routes of infection could be due to the lack of available integrin αvβ6 on the basolateral side, since αvβ6 can bind fibronectin, which is a component of the attachment matrix (48) which was used in our cultures as well.

The most unexpected observation from this experiment was the transient replication of FMDV and absence of any visible sign of CPE, which agrees with the *in vivo* observations in FMDV-infected pig nasal and trachea tissue samples (3; Dash, unpublished). This phenomenon was also observed with another FMDV field isolate of strain OUKG/34/2001. Although extensive CPE characteristic of FMDV infection in conventional monolayer culture was not observed in 3D cultures, the presence of a few floating dead cells could be observed. Their numbers were found to be consistently low at all the time points examined, and any gaps resulting from cell death caused

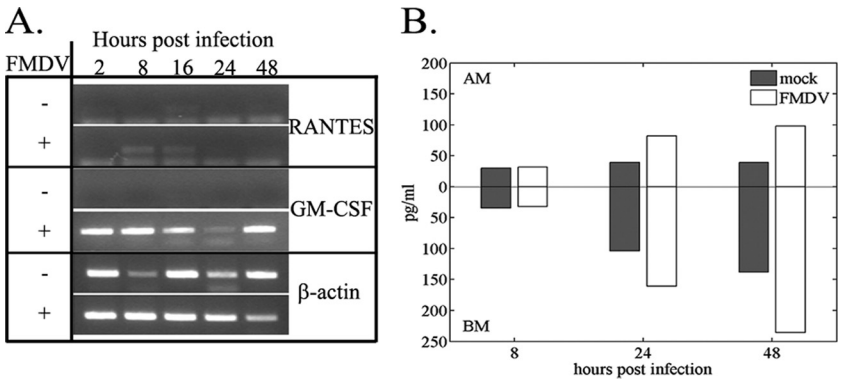

FIG. 6. FMDV infection of 3D nasal mucosal epithelial (NME) cultures induces the IL-8 chemokine and mRNA for RANTES and GM-CSF. (A) RNA samples were prepared from 3D NME cultures either infected with FMDV O1K cad2 (MOI of ~3) (+) or mock infected (−) at various time points, and a standard RT-PCR for a number of chemokines and cytokines was performed. RANTES and GM-CSF were induced in the FMDV-infected cultures. Beta-actin is included as a positive control. (B) Chemokine IL-8 was secreted from both the apical and basolateral sides of both FMDV- and mock-infected cultures as confirmed by a porcine IL-8 ELISA (measured in picograms per milliliter) (B). The mean values from two independent experiments are shown. Although the values were not statistically significantly different, both experiments showed that larger amounts of IL-8 were secreted at the basolateral side of the FMDV-infected cultures at 24 and 48 h postinfection. AM, apical membrane; BM, basolateral membrane.

by FMDV infection in the 3D cultures were not detected, which may be due to the wound-healing properties of the epithelial cells. However, the lack of CPE after FMDV infection is unlikely to be due to a characteristic of the cells or the 3D culture technique alone, since infection of similar cultures with influenza virus results in extensive cytopathology, indicating the involvement of a viral component(s) (P. Dash, P. G. Thomas, and P. C. Doherty [St. Jude Children's Research Hospital], unpublished observations). Noncytopathic virus replication at polarized epithelial cells seems not to be unique to FMDV, as the lack of cytopathology in human airway polarized epithelial cultures infected with respiratory syncytial virus and human parainfluenza virus 3 has also been reported (50, 51). At this time, we do not know what mechanism(s) is/are involved for FMDV nonlytic replication/release in 3D epithelial cells, and further investigation is needed in this regard.

We hypothesized that type I IFN is likely involved in the limited, or transient, replication of FMDV in 3D epithelial cell cultures. Although the level of IFN-α mRNA did not change across the time points appreciably, IFN-β mRNA was demonstrated to be upregulated between 4 to 24 h after FMDV infection, coinciding with the reduction and disappearance of the FMDV mRNA (Fig. 5A and B). Consistent with the induction of IFN-β mRNA, the level of antiviral activity in the supernatant at the 24-h time point of infection of 3D nasal epithelial cultures was significantly higher ($P < 0.047$; Fig. 5D) than in the uninfected culture supernatant. It has been reported that infection of conventional cell cultures by FMDV strain A12 causes a partial blockage of type 1 IFN expression and a reduction of the IFN-stimulated gene products (16). The increased antiviral activity, concurrent with IFN-β mRNA expression, followed by antiviral GTPase Mx1 mRNA expression, indicated that in our system FMDV did not block IFN-β at all or blocked it inefficiently. We do not rule out the role of leader proteinase of FMDV in blocking the IFN; however, in our primary 3D airway epithelial cell culture system, it was not sufficient to completely block IFN-β production. The leader proteinase might be expressed too late to block bystander effects on noninfected neighboring cells, which could then contribute to further IFN secretion and produce a general antiviral state in the culture. This may be due to the constitutive expression of low levels of IFN-α in these 3D cultures and resulting enhanced TLR3 expression. The constitutive expression of IFN-α in 3D nasal epithelial cultures (Fig. 5A) is probably not an *in vitro* artifact, as this was also observed *in vivo*, but it was not expressed in snout tissue samples from the same pigs (data not shown). This observation is supported by publications describing constitutive expression of type I IFN mRNA in human (42) and mouse tissue (46), including the expression in well-differentiated airway epithelia (9). However, the significance of constitutive expression of IFN-α in FMDV infection is not clear, as there are about 14 genes for IFN-α in pigs (12), and at the time of the experiment, only sequence data for IFN-α1 (GenBank accession number M28623) (28) were available. In order to determine the roles of IFN-α and IFN-β during FMDV infection in 3D cultures and/or other factors that might be involved in the limited or transient replication of FMDV observed, we will need to use different approaches, such as small interfering RNA (siRNA) or gene knockout models.

In addition to the type I IFN described above, FMDV infection in 3D epithelial cultures induced GM-CSF and RANTES mRNA, as well as the IL-8 protein (Fig. 6). IL-8 and RANTES are potent chemoattractants (7, 34) and can recruit IFN-γ-producing lymphocytes to the site of FMDV infection. Since IFN-γ is reported to be able to clear persistent FMDV infection (53), these chemokines might have an important role to play in modulating immune response *in vivo*. In fact, increased transmigration of leukocytes in FMDV-infected 3D cultures was observed in a preliminary experiment (data not shown). Although further experiments are needed, these studies indicate that the respiratory mucosal site is much more resilient to FMDV infection than indicated by conventional epithelial cell cultures and may even be triggering rapid innate immune responses to prevent FMDV replication and dissem-

ination at the local site and also recruiting lymphocytes to initiate adaptive immune responses in an effective way.

In conclusion, use of porcine 3D epithelial cell cultures demonstrated that FMDV preferentially infects from the apical membrane and replicates transiently and that the progeny virus is released only from the apical side of the polarized mucosal epithelial cells. In addition to the inhibition of progeny FMDV shedding through the basement membrane, these epithelial cells also restrict FMDV replication probably by inducing rapid innate immune responses involving type I IFN. Furthermore, IL-8, RANTES, and GM-CSF initiate antiviral innate and probably adaptive immunity through recruitment of immune cells to the site of FMDV infection. These observations might explain, at least in part, why pigs are relatively resistant to FMDV infection by the aerosol route, but this needs to be supported by similar studies with 3D cultures derived from cattle.

ACKNOWLEDGMENTS

This work was supported by BBSRC (IAH project 0977, 1042) and DEFRA.

We are grateful to Joe Brownlie (Royal Veterinary College) and Geraldine Taylor for support and technical assistance. We thank Sheila Wilsden for supplying primary BTY cells and Simon Gubbins for designing graphs (Fig. 4A and 6B). We thank Meenu Pillai for assistance with Western blotting and Toru Inoue for the EVOM.

REFERENCES

1. **Alexandersen, S., I. Brotherhood, and A. I. Donaldson.** 2002. Natural aerosol transmission of foot-and-mouth disease virus to pigs: minimal infectious dose for strain O1 Lausanne. Epidemiol. Infect. **128:**301–312.
2. **Alexandersen, S., and A. I. Donaldson.** 2002. Further studies to quantify the dose of natural aerosols of foot-and-mouth disease virus for pigs. Epidemiol. Infect. **128:**313–323.
3. **Alexandersen, S., M. B. Oleksiewicz, and A. I. Donaldson.** 2001. The early pathogenesis of foot-and-mouth disease in pigs infected by contact: a quantitative time-course study using TaqMan RT-PCR. J. Gen. Virol. **82:**747–755.
4. **Alexandersen, S., M. Quan, C. Murphy, J. Knight, and Z. Zhang.** 2003. Studies of quantitative parameters of virus excretion and transmission in pigs and cattle experimentally infected with foot-and-mouth disease virus. J. Comp. Pathol. **129:**268–282.
5. **Alexandersen, S., Z. Zhang, A. I. Donaldson, and A. J. Garland.** 2003. The pathogenesis and diagnosis of foot-and-mouth disease. J. Comp. Pathol. **129:**1–36.
6. **Alexandersen, S., Z. Zhang, S. M. Reid, G. H. Hutchings, and A. I. Donaldson.** 2002. Quantities of infectious virus and viral RNA recovered from sheep and cattle experimentally infected with foot-and-mouth disease virus O UK 2001. J. Gen. Virol. **83:**1915–1923.
7. **Asselin-Paturel, C., G. Brizard, K. Chemin, A. Boonstra, A. O'Garra, A. Vicari, and G. Trinchieri.** 2005. Type I interferon dependence of plasmacytoid dendritic cell activation and migration. J. Exp. Med. **201:**1157–1167.
8. **Berinstein, A., M. Roivainen, T. Hovi, P. W. Mason, and B. Baxt.** 1995. Antibodies to the vitronectin receptor (integrin alpha V beta 3) inhibit binding and infection of foot-and-mouth disease virus to cultured cells. J. Virol. **69:**2664–2666.
9. **Bielenberg, D. R., I. J. Fidler, and C. D. Bucana.** 1998. Constitutive expression of interferon beta in differentiated epithelial cells exposed to environmental stimuli. Cancer Biother. Radiopharm. **13:**375–382.
10. **Brown, J. K., S. M. McAleese, E. M. Thornton, J. A. Pate, A. Schock, A. I. Macrae, P. R. Scott, H. R. Miller, and D. D. Collie.** 2006. Integrin-alphavbeta6, a putative receptor for foot-and-mouth disease virus, is constitutively expressed in ruminant airways. J. Histochem. Cytochem. **54:**807–816.
11. **Callis, J. J., and D. A. Gregg.** 1994. Foot and mouth disease, p. 9. *In* G. W. Beran (ed.), Handbook of zoonoses, 2nd ed. Section B: Viral. CRC Press LLC, Boca Raton, FL.
12. **Cheng, G., W. Chen, Z. Li, W. Yan, X. Zhao, J. Xie, M. Liu, H. Zhang, Y. Zhong, and Z. Zheng.** 2006. Characterization of the porcine alpha interferon multigene family. Gene **382:**28–38.
13. **Cordo, S. M., M. Cesio y Acuna, and N. A. Candurra.** 2005. Polarized entry and release of Junin virus, a New World arenavirus. J. Gen. Virol. **86:**1475–1479.
14. **Crook, T. J., I. S. Hall, L. Z. Solomon, B. R. Birch, and A. J. Cooper.** 2000. A model of superficial bladder cancer using fluorescent tumour cells in an organ-culture system. BJU Int. **86:**886–893.
15. **Curry, S., E. Fry, W. Blakemore, R. Abu-Ghazaleh, T. Jackson, A. King, S. Lea, J. Newman, D. Rowlands, and D. Stuart.** 1996. Perturbations in the surface structure of A22 Iraq foot-and-mouth disease virus accompanying coupled changes in host cell specificity and antigenicity. Structure **4:**135–145.
16. **de Los Santos, T., S. de Avila Botton, R. Weiblen, and M. J. Grubman.** 2006. The leader proteinase of foot-and-mouth disease virus inhibits the induction of beta-interferon mRNA and blocks the host innate immune response. J. Virol. **80:**1906–1914.
17. **Donaldson, A. I., and S. Alexandersen.** 2002. Predicting the spread of foot and mouth disease by airborne virus. Rev. Sci. Tech. **21:**569–575.
18. **Esni, F., Y. Miyamoto, S. D. Leach, and B. Ghosh.** 2005. Primary explant cultures of adult and embryonic pancreas. Methods Mol. Med. **103:**259–271.
19. **Fahey, J. V., T. M. Schaefer, J. Y. Channon, and C. R. Wira.** 2005. Secretion of cytokines and chemokines by polarized human epithelial cells from the female reproductive tract. Hum. Reprod. **20:**1439–1446.
20. **Fray, M. D., G. E. Mann, and B. Charleston.** 2001. Validation of an Mx/CAT reporter gene assay for the quantification of bovine type-I interferon. J. Immunol. Methods **249:**235–244.
21. **Glorieux, S., W. Van den Broeck, K. M. van der Meulen, K. Van Reeth, H. W. Favoreel, and H. J. Nauwynck.** 2007. In vitro culture of porcine respiratory nasal mucosa explants for studying the interaction of porcine viruses with the respiratory tract. J. Virol. Methods **142:**105–112.
22. **Jackson, T., S. Clark, S. Berryman, A. Burman, S. Cambier, D. Mu, S. Nishimura, and A. M. King.** 2004. Integrin alphavbeta8 functions as a receptor for foot-and-mouth disease virus: role of the beta-chain cytodomain in integrin-mediated infection. J. Virol. **78:**4533–4540.
23. **Jackson, T., A. P. Mould, D. Sheppard, and A. M. King.** 2002. Integrin alphavbeta1 is a receptor for foot-and-mouth disease virus. J. Virol. **76:**935–941.
24. **Jackson, T., D. Sheppard, M. Denyer, W. Blakemore, and A. M. King.** 2000. The epithelial integrin alphavbeta6 is a receptor for foot-and-mouth disease virus. J. Virol. **74:**4949–4956.
25. **Kim, J. M., Y. K. Oh, Y. J. Kim, H. B. Oh, and Y. J. Cho.** 2001. Polarized secretion of CXC chemokines by human intestinal epithelial cells in response to Bacteroides fragilis enterotoxin: NF-kappa B plays a major role in the regulation of IL-8 expression. Clin. Exp. Immunol. **123:**421–427.
26. **Korn, G.** 1957. Experimental studies of the demonstration of virus during the incubation period of foot-and-mouth disease and of its pathogenesis. Arch. Exp. Vet. Med. **11:**637–649.
27. **La Rocca, S. A., R. J. Herbert, H. Crooke, T. W. Drew, T. E. Wileman, and P. P. Powell.** 2005. Loss of interferon regulatory factor 3 in cells infected with classical swine fever virus involves the N-terminal protease, Npro. J. Virol. **79:**7239–7247.
28. **Lefevre, F., and C. La Bonnardiere.** 1986. Molecular cloning and sequencing of a gene encoding biologically active porcine alpha-interferon. J. Interferon Res. **6:**349–360.
29. **Logan, D., R. Abu-Ghazaleh, W. Blakemore, S. Curry, T. Jackson, A. King, S. Lea, R. Lewis, J. Newman, N. Parry, et al.** 1993. Structure of a major immunogenic site on foot-and-mouth disease virus. Nature **362:**566–568.
30. **McCahon, D., J. R. Crowther, G. J. Belsham, J. D. Kitson, M. Duchesne, P. Have, R. H. Meloen, D. O. Morgan, and F. De Simone.** 1989. Evidence for at least four antigenic sites on type O foot-and-mouth disease virus involved in neutralization: identification by single and multiple site monoclonal antibody-resistant mutants. J. Gen. Virol. **70:**639–645.
31. **Mellow, T. E., P. C. Murphy, J. L. Carson, T. L. Noah, L. Zhang, and R. J. Pickles.** 2004. The effect of respiratory syncytial virus on chemokine release by differentiated airway epithelium. Exp. Lung Res. **30:**43–57.
32. **Moffat, K., G. Howell, C. Knox, G. J. Belsham, P. Monaghan, M. D. Ryan, and T. Wileman.** 2005. Effects of foot-and-mouth disease virus nonstructural proteins on the structure and function of the early secretory pathway: 2BC but not 3A blocks endoplasmic reticulum-to-Golgi transport. J. Virol. **79:**4382–4395.
33. **Monaghan, P., S. Gold, J. Simpson, Z. Zhang, P. H. Weinreb, S. M. Violette, S. Alexandersen, and T. Jackson.** 2005. The alpha(v)beta6 integrin receptor for foot-and-mouth disease virus is expressed constitutively on the epithelial cells targeted in cattle. J. Gen. Virol. **86:**2769–2780.
34. **Moser, B., M. Wolf, A. Walz, and P. Loetscher.** 2004. Chemokines: multiple levels of leukocyte migration control. Trends Immunol. **25:**75–84.
35. **Mu, D., S. Cambier, L. Fjellbirkeland, J. L. Baron, J. S. Munger, H. Kawakatsu, D. Sheppard, V. C. Broaddus, and S. L. Nishimura.** 2002. The integrin alpha(v)beta8 mediates epithelial homeostasis through MT1-MMP-dependent activation of TGF-beta1. J. Cell Biol. **157:**493–507.
36. **Newby, C. M., R. K. Rowe, and A. Pekosz.** 2006. Influenza A virus infection of primary differentiated airway epithelial cell cultures derived from Syrian golden hamsters. Virology **354:**80–90.
37. **Roskelley, C. D., and M. J. Bissell.** 1995. Dynamic reciprocity revisited: a continuous, bidirectional flow of information between cells and the extracellular matrix regulates mammary epithelial cell function. Biochem. Cell Biol. **73:**391–397.
38. **Sellers, R. F., and J. Parker.** 1969. Airborne excretion of foot-and-mouth disease virus. J. Hyg. (Lond.) **67:**671–677.
39. **Sims, A. C., R. S. Baric, B. Yount, S. E. Burkett, P. L. Collins, and R. J.**

Pickles. 2005. Severe acute respiratory syndrome coronavirus infection of human ciliated airway epithelia: role of ciliated cells in viral spread in the conducting airways of the lungs. J. Virol. **79:**15511–15524.
40. **Snowdon, W. A.** 1966. Growth of foot-and mouth disease virus in monolayer cultures of calf thyroid cells. Nature **210:**1079–1080.
41. **Steinert, P. M., and D. R. Roop.** 1988. Molecular and cellular biology of intermediate filaments. Annu. Rev. Biochem. **57:**593–625.
42. **Tovey, M. G., M. Streuli, I. Gresser, J. Gugenheim, B. Blanchard, J. Guymarho, F. Vignaux, and M. Gigou.** 1987. Interferon messenger RNA is produced constitutively in the organs of normal individuals. Proc. Natl. Acad. Sci. U. S. A. **84:**5038–5042.
43. **Tran, S. D., J. Wang, B. C. Bandyopadhyay, R. S. Redman, A. Dutra, E. Pak, W. D. Swaim, J. A. Gerstenhaber, J. M. Bryant, C. Zheng, C. M. Goldsmith, M. R. Kok, R. B. Wellner, and B. J. Baum.** 2005. Primary culture of polarized human salivary epithelial cells for use in developing an artificial salivary gland. Tissue Eng. **11:**172–181.
44. **Tseng, C. T., J. Tseng, L. Perrone, M. Worthy, V. Popov, and C. J. Peters.** 2005. Apical entry and release of severe acute respiratory syndrome-associated coronavirus in polarized Calu-3 lung epithelial cells. J. Virol. **79:**9470–9479.
45. **Tugizov, S. M., J. W. Berline, and J. M. Palefsky.** 2003. Epstein-Barr virus infection of polarized tongue and nasopharyngeal epithelial cells. Nat. Med. **9:**307–314.
46. **van Pesch, V., and T. Michiels.** 2003. Characterization of interferon-alpha 13, a novel constitutive murine interferon-alpha subtype. J. Biol. Chem. **278:**46321–46328.
47. **Wang, G., C. Deering, M. Macke, J. Shao, R. Burns, D. M. Blau, K. V. Holmes, B. L. Davidson, S. Perlman, and P. B. McCray, Jr.** 2000. Human coronavirus 229E infects polarized airway epithelia from the apical surface. J. Virol. **74:**9234–9239.
48. **Weinacker, A., R. Ferrando, M. Elliott, J. Hogg, J. Balmes, and D. Sheppard.** 1995. Distribution of integrins alpha v beta 6 and alpha 9 beta 1 and their known ligands, fibronectin and tenascin, in human airways. Am. J. Respir. Cell Mol. Biol. **12:**547–556.
49. **Yamaya, M., W. E. Finkbeiner, S. Y. Chun, and J. H. Widdicombe.** 1992. Differentiated structure and function of cultures from human tracheal epithelium. Am. J. Physiol. **262:**L713–L724.
50. **Zhang, L., A. Bukreyev, C. I. Thompson, B. Watson, M. E. Peeples, P. L. Collins, and R. J. Pickles.** 2005. Infection of ciliated cells by human parainfluenza virus type 3 in an in vitro model of human airway epithelium. J. Virol. **79:**1113–1124.
51. **Zhang, L., M. E. Peeples, R. C. Boucher, P. L. Collins, and R. J. Pickles.** 2002. Respiratory syncytial virus infection of human airway epithelial cells is polarized, specific to ciliated cells, and without obvious cytopathology. J. Virol. **76:**5654–5666.
52. **Zhang, Z., and S. Alexandersen.** 2004. Quantitative analysis of foot-and-mouth disease virus RNA loads in bovine tissues: implications for the site of viral persistence. J. Gen. Virol. **85:**2567–2575.
53. **Zhang, Z. D., G. Hutching, P. Kitching, and S. Alexandersen.** 2002. The effects of gamma interferon on replication of foot-and-mouth disease virus in persistently infected bovine cells. Arch. Virol. **147:**2157–2167.